J. Membrane Biol. 96, 75–84 (1987)

The Journal of
Membrane Biology

Role of Calcium Ion in the Excitability and Electrogenic Pump Activity of the *Chara corallina* Membrane: II. Effects of La^{3+}, EGTA, and Calmodulin Antagonists on the Current-Voltage Relation

Izuo Tsutsui, Taka-aki Ohkawa, Reiko Nagai, and Uichiro Kishimoto
Department of Biology, College of General Education, Osaka University, Toyonaka 560, Osaka, Japan

Summary. The steady N shape *I/V* curves were obtained by applying slow ramp hyper- and depolarization pulses to *Chara* cells under the voltage-clamp condition. Application of calcium channel blocker, 20 μM La^{3+}, to the *Chara* membrane caused, in about 30 min, a marked reduction of the transient inward current and later almost complete blocking of the pump current, while the steady outward current remained almost unaffected. Removal of external Ca^{2+} with 0.5 mM EGTA caused similar results. Application of calmodulin antagonists, 10 μM TFP or 20 μM W-7, also gave very similar results, i.e., the decrease of the transient inward current and of H^+-pump activity. These results suggest that not only the excitatory mechanisms but also the H^+-pump activity of *Chara* membrane are regulated by calmodulin within a comparatively narrow range of internal Ca^{2+} level.

Key Words Ca^{2+} activation · Ca^{2+} channel · calmodulin · electromotive force · H^+ pump · *I/V* curve

Introduction

In the *Chara* membrane the N-shaped current-voltage (*I/V*) curve was caused mainly by the initial transient increase of Cl^- efflux and later increase of K^+ efflux (Gaffey & Mullins, 1958; Kishimoto, 1961; 1964; 1965; 1968; Mullins, 1962; Mailman & Mullins, 1965; Kitasato, 1973; Oda, 1976). Findlay and Hope (1964) suggested a possible role of external Ca^{2+} for the generation of transient current during the voltage clamp. Beilby and Coster (1979) suggested that a part of early transient current might be carried by the inward movement of Ca^{2+} under the voltage-clamp condition. Hayama, Shimmen and Tazawa (1979) found the increase of $^{45}Ca^{2+}$ influx in proportion to the number of stimuli. The increase of internal Ca^{2+} during an action potential was detected by the increase of fluorescence of internally loaded aequorin (Williamson & Ashley, 1982; Kikuyama & Tazawa, 1983). Lunevsky et al. (1983) and Tsutsui et al. (1987) suggested activation of Cl^- channel of the *Chara* membrane by Ca^{2+}. It is well-known that Ca^{2+} acts as a co-factor of the Ca^{2+}-dependent regulator such as calmodulin. Activation of the passive channels via the Ca^{2+}-calmodulin system is also suggested by Beilby and MacRobbie (1984). In this report we introduce the results which indicate that not only activation of the Cl^- channel but also activity of the H^+ pump of the *Chara* membrane are regulated within a narrow range of internal Ca^{2+} concentration.

Materials and Methods

Giant internodal cells of *Chara corallina* were used throughout the experiment. The average diameter of internodes used was about 0.7 mm and 4 to 6 cm in length. The artificial pond water (APW) contained (in mM) 0.5 KCl, 0.1 NaCl, 0.1 $Ca(NO_3)_2$ and 0.2 $Mg(NO_3)_2$, the pH of which was adjusted at 7.0 with 2.0 mM TES.

We used La^{3+} as a Ca^{2+}-channel blocker (Lettvin et al., 1964; Takata et al., 1966), EGTA as a calcium chelating agent, TFP (Levin & Weiss, 1976) and W-7 (Hidaka & Tanaka, 1983) as calmodulin antagonists.

The *Chara* membrane has two independent ionic pathways, one being the electrogenic H^+ pump and another the passive diffusion channel. Also, there is a possibility of the existence of other primary or secondary transport systems such as Ca^{2+} pump (*see* a review by Schatzmann, 1982) H^+/Cl^- cotransport (Sanders, 1980), Ca^{2+}/H^+ antiport (Hager, Menzel & Krauss, 1971), HCO_3^-/Cl^- antiport (Boron et al., 1978), other H^+/anion cotransport system (*see* a review by Sze, 1985) and so on. If these are electroneutral, they will not contribute to the current actually measured. Even if these are electrogenic, the contribution of these transport system to the *I/V* relation of *Chara corallina* internode is expected to be minor, judging from the published data. The simplest way for describing this situation is to adopt an equivalent circuit, shown in Fig. 1, as a membrane model. The membrane conductance is the sum of the conductance (g_d) of the passive channel and the conductance (g_p) of the H^+ pump. The resting potential or the electromotive force (emf), E, of the *Chara* membrane is the weighted average of two emf's, i.e., E_d (passive channel) and E_p (H^+ pump), weights being conductances (g_d and g_p) of each channel. Membrane current I is the

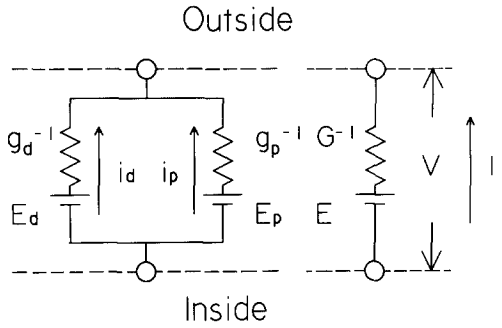

Fig. 1. A circuit model for the *Chara* membrane having an electrogenic pump system in parallel with the passive channel.

sum of i_d and i_p, which are the currents flowing through the passive and the H^+ pump channels, respectively. These relations are described with the following equations:

$$i_p = g_p(V - E_p) \quad (1)$$

$$i_d = g_d(V - E_d) \quad (2)$$

$$I = i_p + i_d = G(V - E) \quad (3)$$

where

$$G = g_p + p_d \quad (4)$$

and

$$E = (g_pE_p + g_dE_d)/G. \quad (5)$$

To study the detailed electrical property of *Chara* membrane, we measured the current-voltage curves (I/V curves). The I/V curve was obtained bv applying a slow ramp hyperpolarization first, followed by a slow ramp depolarization under the voltage-clamp condition (Kishimoto et al., 1984; 1985; Takeuchi et al., 1985). Furthermore, small square test pulses (ΔV) were superimposed repeatedly on the ramp voltage-clamp condition to evaluate the membrane chord conductance and the electromotive force as functions of voltage (Ohkawa & Kishimoto, 1974; 1977; Kishimoto et al., 1984). The duration of the superimposed pulses was long (40 msec) enough to obtain a steady-state current response (ΔI). The ΔV was small enough and did not affect the membrane emf, E, appreciably. Thus, the conductance G was evaluated from the ratio of the amplitude of current ΔI to that of potential ΔV. Since I and G are known, E for various membrane potential levels can be calculated with Eq. (3). The internodal cells were perfused externally with APW or with test solutions at a rate of 1 liter/hr. Acquisition of the data and calculation of the electrical characteristics were performed with a CP/M-80 microcomputer system. The details of data processing have previously been reported by Kishimoto et al. (1981; 1984).

Abbreviations

EGTA, glycoletherdiamine-N,N,N',N'-tetraacetic acid; W-7, N-(6-aminohexyl)-5-chloro-1-naphthalenesulfonamide; TFP (trifluroperadine), 3-trifluoromethyl-10-(3-(4-methyldipiperazinyl)-propyl)-phenothiazine dihydrates; DCCD, dicyclohexylcarbodiimide; TES, N-Tris(hydroxymethyl)-methyl-2-aminoethanesulfonic acid; emf, electromotive force

Results

I/V Characteristics Obtained with the Slow Ramp Voltage-Clamp Method

The I/V curves obtained with different rates of ramp are compared with Fig. 2*A*. Except for the location of the transient current region, these I/V curves are practically the same as the steady state I/V relation which is obtained with the conventional step voltage-clamp method, if the ramp rate is slower than 100 mV/30 sec. The obtained I/V curve of the *Chara* membrane is nonlinear and generally consists of three voltage regions, i.e., around the resting and more negative voltage range with low conductance (region I), large depolarization range with high conductance (region III) and the region in between regions I and III with transient current and high conductance (region II). The transient current region shifts along the voltage axis, depending on the rate of ramp. In spite of the difference between these I/V curves in the transient current region, the emf at the peak of the inward current (Epeak) obtained by the ramp voltage-clamp method, agreed with that obtained by the step voltage clamp. This emf corresponds to the peak of action potential. The threshold level is defined in this report as the voltage where dV/dI changes its sign (Eth in Fig. 2*A*). The emf at the late steady high conductance region obtained by the ramp voltage-clamp method coincides with the one obtained by the step voltage clamp (Est in Fig. 2*A*). It is worth noting that Est is dependent on voltage. The conductance at any voltage (full line in Fig. 2*B*), obtained by the slow ramp voltage-clamp method (the rate of ramp; 100 mV/30 sec), showed a satisfactory agreement with the one (filled circles in Fig. 2*B*) obtained by the step voltage clamp. The resting potential (RP), the threshold level (Eth) and the emf (Epeak) at the peak of transient inward current are about −205, −120 and −30 mV, respectively, in the normal *Chara* membrane. The emf in region III is about −130 mV and remained unchanged for voltage change (Est in Fig. 2*A*) as described above.

Effect of DCCD

The I/V curve of the control internode of *Chara corallina* under the ramp voltage clamp was a typi-

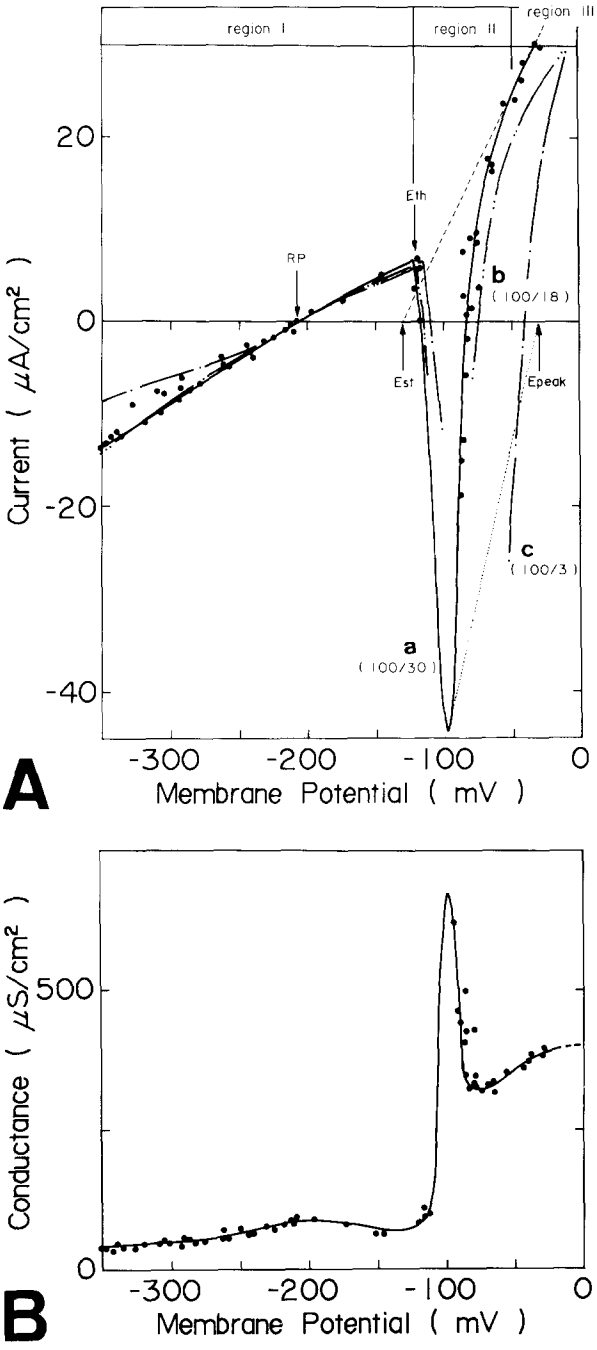

Fig. 2. (*A*) The *I/V* relations which are recorded with a slow ramp and a step voltage-clamp method. *a*, *b* and *c* are the *I/V* curves obtained at different rates of ramp voltage clamp, i.e., 100/30, 100/18 and 100/3 (mV/sec), respectively. Symbols (●) are the steady-state currents as functions of step voltage changes. These steady-state currents in the voltage range less negative than −50 mV and more negative than threshold level are on the *I/V* curve obtained by the ramp voltage clamp, the ramp rate of which is slower than 100 mV/30 sec. The extrapolation of the broken line to the voltage axis in region III (Est = −130 mV) represents the electromotive force in this region. The extrapolation of the dotted line at the peak of transient inward current to the voltage axis (E_{peak}) corresponds to the peak level of action potential. (*B*) Curve represents the *G/V* curve at ramp rate as 100/30 (mV/sec). Symbols (●) are the data of conductance obtained by step clamp. The smaller peak of the conductance at about −200 mV is caused by the peak conductance of H^+ pump. Another much larger conductance peak at about −100 mV (= 675 μS/cm²) corresponds to that at the peak of the excitation of the passive channel

cal N-shaped one. Kishimoto et al. (1984) reported on the effect of DCCD on the i_p/V curve of the electrogenic H^+ pump in the voltage range more negative than the threshold level. Here, we studied the effect of DCCD on the parts including the transient current region and the steady high conductance region. The resting potential before the application of DCCD was −216 mV (RP(a)) and the threshold level was −116 mV (Est(a) in Fig. 3*A*). The transient inward current region in this N-shaped *I/V* curve was caused by a transient depolarization of the membrane emf (Kishimoto, 1968). This depolarization was caused mainly by the marked increases of Cl^- and K^+ conductances as described above. The emf at the peak inward current was −40 mV (Epeak(a) in FIg. 3*A*). The emf in region III was almost constant at −140 mV (Est(a) in Fig. 3*A*). On the other hand, the *G/V* curve had two peaks, the one (160 μS/cm²) at about −200 mV, is caused by the peak conductance of the electrogenic pump (Kishimoto et al., 1984; 1985), while the other (650 μS/cm²) at −110 mV, is caused by the excitation of the passive channel (curve *a* in Fig. 3*B*).

DCCD can be regarded as an ideal inhibitor for the H^+ pump in the *Chara* membrane, leaving the excitability of the passive channels almost unaffected (Kishimoto et al., 1984; 1985). The same internode was perfused externally with DCCD-APW (75 μM DCCD). In about 2 hr the *I/V* curve reached a steady i_d/V curve of the passive channel (curve *b* in Fig. 3*A*). The resting potential depolarized from −216 mV to the level of the passive diffusion potential asymptotically (about −136 mV: RP(b) in Fig. 3*A*). The transient inward current component was reduced only slightly. There was slight depolarization of the threshold level (around −112 mV: Eth(b) in Fig. 3*A*) by DCCD treatment. The emf at the peak inward current was almost unchanged (−40 mV) with DCCD treatment (Epeak(b) in Fig. 3*A*). The emf in region III was −120 mV (Est(b)). This was about 20 mV depolarization compared with the one obtained before inhibition (Est(a)).

The H^+-pump activity of the plasmalemma was diminished to almost zero in about 2 hr by DCCD poisoning, which is indicated by the loss of the peak of the *G/V* curve at around −200 mV (curve *b* in Fig. 3*B*). The *G/V* curve at this stage is supposed to correspond to the g_d/V curve of the passive chan-

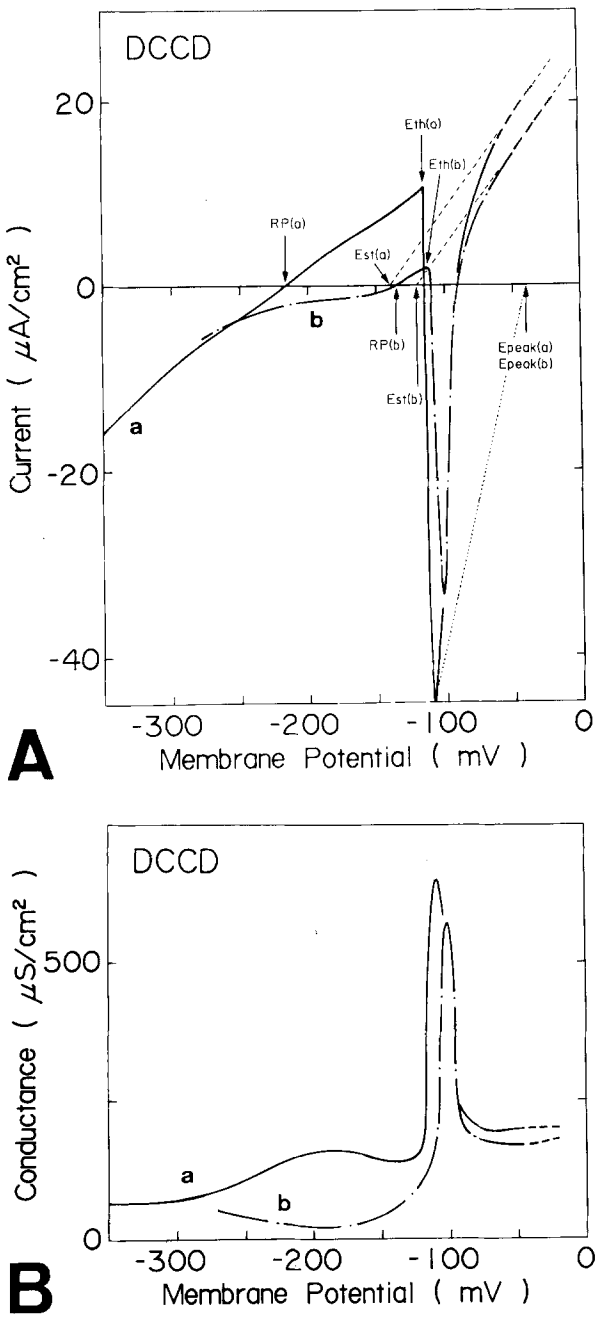

Fig. 3. (*A*) Changes of *I/V* curve with 75 μM DCCD. (*a*) The *I/V* curve of the normal *Chara* membrane. (*b*) The *I/V* curve recorded after 2-hr treatment with 75 μM DCCD. The resting potential was depolarized by about 80 mV. The transient inward current was not decreased much after 2-hr treatment with DCCD. The electromotive force of region III, Est(a), is −140 mV in curve *a*. Est(b) after poisoning with DCCD is −120 mV (Est(b) in *b*). (*B*) *a* and *b* are the *G/V* curves before and after DCCD (75 μM) treatment, respectively. A smaller peak of the conductance at about −200 mV is caused by the peak of conductance of the H^+ pump. This peak was markedly reduced after 2-hr DCCD treatment. Another much larger conductance peak at about −100 mV, which corresponds to that at the peak of excitation of the passive channel, shows no marked decrease with DCCD treatment. The conductance of region III, where the voltage is less negative than −50 mV, remained almost unaffected

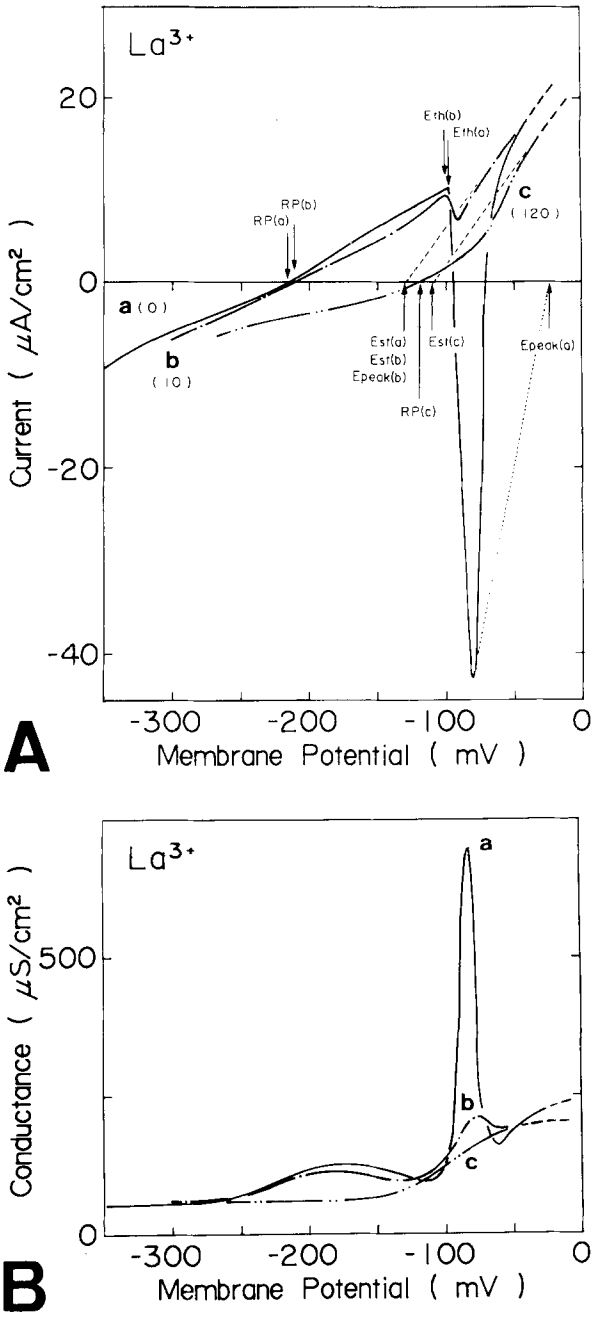

Fig. 4. (*A*) Changes of *I/V* curve with 20 μM La^{3+}. The *I/V* curves are obtained before (*a*), 10 min (*b*) and 2 hr (*c*) after application of La^{3+}. The transient inward current decreased markedly in *b* without a marked change in resting potential (RP(b)). However, in 2 hr the resting potential was depolarized to a great extent (RP(c)) and the transient inward current disappeared completely. The emf in region III (Est) is shown with the extrapolation of broken lines to the voltage axis. The Est is about −130 mV in *a* and in *b*, while it is about −110 mV in *c*. (*B*) The *G/V* curves obtained before (*a*), 10 min (*b*) and 2 hr (*c*) after the application of 20 μM La^{3+}. The conductance peak at around −180 mV corresponds to the peak conductance of the H^+ pump, while the larger one at around −85 mV to that of the passive excitatory channels. Note that the latter decreased markedly without marked decrease of the former in *b*. On the other hand, both conductance peaks disappeared in *c*

nel. On the other hand, another peak conductance corresponding to the peak inward current through the passive channel remained at about −103 mV with only a slight decrease (570 μS/cm^2). This supports the previous assumption that DCCD is an almost ideal inhibitor of the H^+ pump.

Effect of Calcium Channel Blocking

External perfusion with La^{3+}-APW (20 μM La^{3+}) caused a marked loss of the transient inward current component in about 10 min. On the other hand, the effect of La^{3+} on the pump progressed very slowly and finally blocked the pump in about 2 hr.

Early Effect

No significant change of the resting potential (RP(b)) and the threshold level (Eth(b)) were observed at the early stage of La^{3+} treatment (curves *a* and *b* in Fig. 4*A*), while the transient inward current was markedly reduced (curve *b* in Fig. 4*A*). The emf at the peak of transient inward current shifted from −23 mV (Epeak(a)) to −130 mV (Epeak(b)). This corresponds to a marked decrease of the amplitude of action potential (Tsutsui et al., 1987). On the other hand, the emf in region III was −130 mV (Est(b)), which is almost the same as the one (Est(a)) obtained before inhibition. The peak of conductance at around −180 mV was not reduced, while that at around −84 mV was depressed markedly (curve *b* in Fig. 4*B*) at this stage. This state lasted for about 1 hr.

Late Effect

In about 2 hr of continuous perfusion with La^{3+}-APW the *I/V* curve reached another steady state (curve *c* in Fig. 4*A*). The resting potential depolarized from −220 mV (RP(a)) to −120 mV (RP(c)). The transient inward current component was lost completely (curve *c* in Fig. 4*A*). The emf of region III was −110 mV (Est(c)), which depolarized about −20 mV from the level (Est(a)) before inhibition.

The H^+-pump activity of the plasmalemma which is indicated by a peak of *G/V* curve at about −180 mV (curve *c* in Fig. 4*B*) was also lost completely in the late stage of La^{3+} treatment. No recovery of the transient inward current component was observed by the external perfusion with Ca^{2+}-APW (3 mM $CaCl_2$, *data not shown*). Verapamil (another Ca^{2+} channel blocker) at 100 μM caused very similar effects on the *I/V*, *G/V* curves and on the emf at the peak of transient inward current (*data not shown*).

Effect of External Calcium Deficiency

Another internode was perfused externally with EGTA-APW (0.5 mM EGTA) for about 27 min to cause an external free Ca^{2+} deficiency in the *Chara* plasma membrane. The concentration of the free Ca^{2+} in the external EGTA-APW is expected to be as low as 10^{-8} M. The resting potential depolarized from −186 mV (RP(a)) to −136 mV (RP(b) in Fig. 5*A*). The transient inward current reduced markedly and the threshold level shifted from −111 mV (Eth(a)) to −82 mV (Eth(b) in Fig. 5*A*). The emf at the peak of transient inward current shifted from −22 mV (Epeak(a)) to −40 mV (Epeak(b) in Fig. 5*A*), which corresponds to the decrease of the size of the action potential to less than half (Tsutsui et al., 1987). The emf in region III was −110 mV (Est(b)), which is about 21 mV depolarization from the one before inhibition (Est(a)).

The H^+-pump activity of the plasmalemma was diminished markedly by EGTA treatment. This was judged from the result that the peak of the *G/V* curve at around −180 mV was lost (curve *b* in Fig. 5*B*). The effect of EGTA could mostly be removed by washing the *Chara* internode with 1 mM Ca^{2+}-APW (*data not shown*).

Effect of Calmodulin Antagonists

We tested the effects of two different types of calmodulin antagonists (one being phenotiazine type TFP and another aminonaphthalene type W-7) on the electrical characteristics of the *Chara* membrane.

TFP

The internode was perfused externally with TFP-APW (10 μM TFP). The resting potential depolarized markedly from −230 mV (RP(a)) to −158 mV (RP(b)) in about 25 min. The threshold level depolarized from −118 mV (Eth(a)) to −104 mV (Eth(b) in Fig. 6*A*). The transient inward current component decreased markedly with TFP treatment. The emf at the peak of the transient inward current shifted from −30 mV (Epeak(a)) to −36 mV (Epeak(b) in Fig. 6*A*). This corresponds to the decrease of the size of action potential (Tsutsui et al., 1987). In spite of the marked change in *I/V* curve, the emf in region III (Est(b)) remained at −130 mV, which is about 20 mV less negative than that before inhibition (Est(a) in Fig. 6*A*).

The H^+-pump activity of the plasmalemma was reduced markedly by TFP poisoning as indicated by the loss of peak of the *G/V* curve at around −200 mV. Another peak of the conductance at around

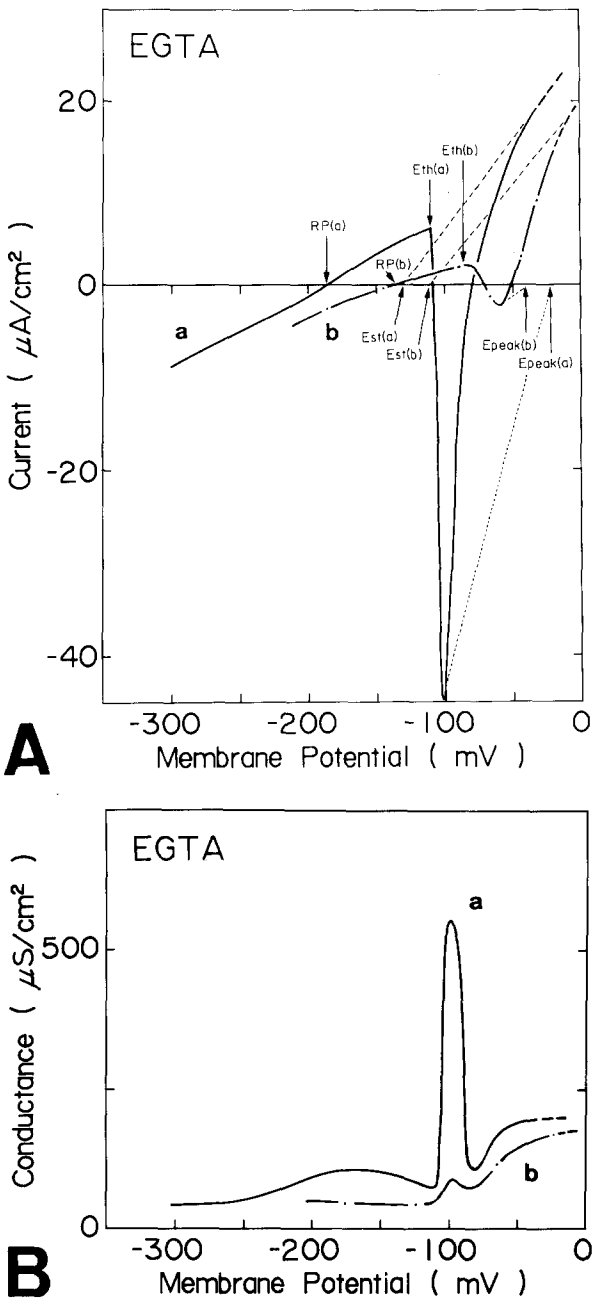

Fig. 5. (*A*) Changes of *I/V* curve with 0.5 mM EGTA. The *I/V* curves obtained before (*a*) and 27 min after (*b*) the application of EGTA. The resting potential depolarized markedly (RP(b)) in *b*. The transient inward current decreased markedly and the threshold level (Eth(b)) shifted to a less negative level in *b*. The Est in region III is about −130 mV in *a* and −110 mV in *b*. (*B*) The *G/V* curves obtained before (*a*) and 27 min after (*b*) the application of EGTA (0.5 mM). A smaller conductance peak at around −180 mV corresponds to the peak conductance of H^+ pump, while the larger one at around −104 mV corresponds to that of the passive excitatory channel. Both conductance peaks reduced markedly in *b*. The conductance of the late steady high conductance region, where voltage is less negative than −50 mV was affected not much by EGTA in *b*

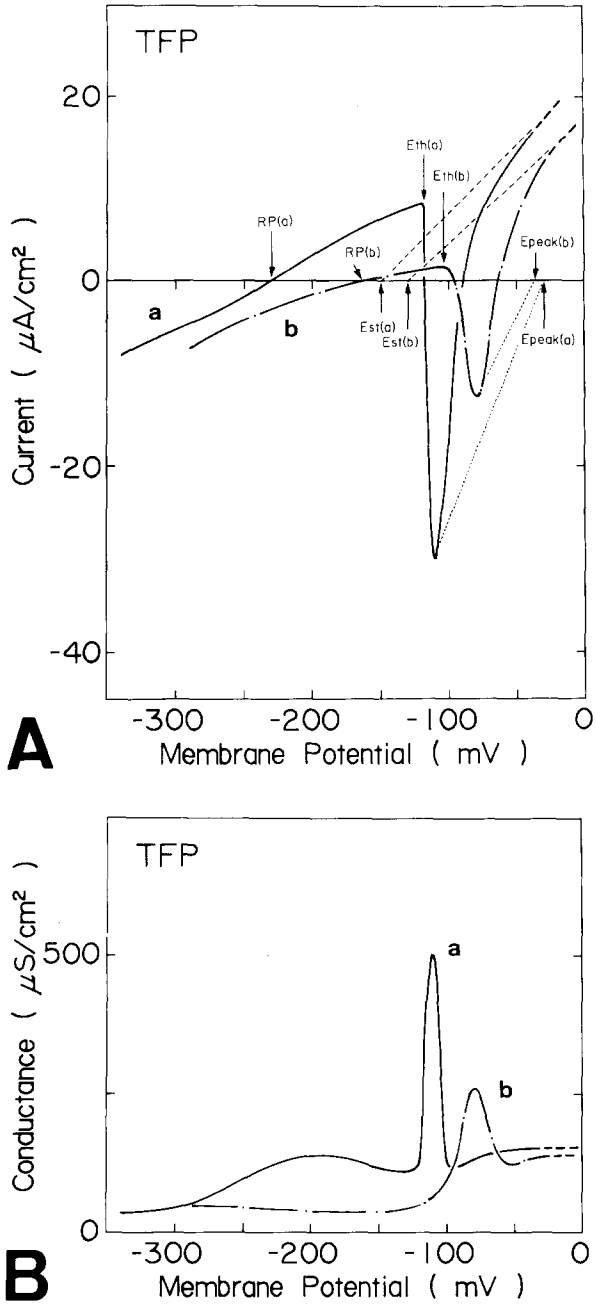

Fig. 6. (*A*) Changes of *I/V* curve with 10 μM TFP. The *I/V* curves obtained before (*a*) and 25 min after (*b*) the application of TFP. The resting potential depolarized markedly (RP(b)) in *b*. The transient inward current decreased markedly and the threshold level (Eth(b)) shifted to a less negative level in *b*. The emf of region III (Est) is about −150 mV in *a* and −130 mV in *b*. (*B*) The *G/V* curves obtained before (*a*) and 25 min after (*b*) application of TFP (10 μM). The smaller conductance peak at around −200 mV corresponds to the peak conductance of H^+ pump, while the larger one at around −112 mV to that of the passive excitatory channel. Both conductance peaks reduced markedly in *b*. The conductance of the late steady high conductance region, where the voltage is less negative than −50 mV was not affected so much by EGTA in *b*

−80 mV reduced down to 270 μS/cm^2 (curve *b* in Fig. 6*B*), which corresponds to the reduction of excitability. The effect of TFP was partly removed by the addition of Ca^{2+} in the external medium (*data not shown*).

W-7

The *I/V* curve of another control internode is shown in Fig. 7*A* curve *a*. The same internode was, then, perfused externally with W-7-APW (20 μM of W-7) for about 50 min. The resting potential depolarized from −211 mV (RP(a)) to −126 mV (RP(b) in Fig. 7*A*). The threshold level depolarized from −132 mV (Eth(a)) to −100 mV (Eth(b) in Fig. 7*A*). The transient current region shifted to the depolarizing direction and the transient current reduced to less than half. The emf at the peak of the transient inward current shifted from −18 mV (Epeak(a)) to −25 mV (Epeak(b) in Fig. 7*A*). The emf in region III was depolarized from −150 mV (Est(a)) to −120 mV (Est(b)).

The H^+-pump activity of the plasmalemma was reduced markedly by W-7 poisoning which is indicated by the loss of peak of the conductance at around −200 mV (curve *b* in Fig. 7*B*). Cells treated with W-7 showed partial recovery, both of the excitability and of the pump activity by the addition of 3 mM Ca^{2+} to the external medium (*data not shown*). These results are very similar to the TFP treatment.

Discussion

The ionic activity of K^+ measured with K^+-selective microelectrode, in *Nitella clavata* and in the cytoplasmic droplet of *Chara australis* are about 61 mM (Kitasato, 1973) and 68 mM (Reeves, Shimmen & Tazawa, 1985), respectively. These were a little smaller than one obtained by measuring the atomic absorbance (Tazawa, Kishimoto & Kikuyama, 1974). If data are correct, the activity coefficient for K^+ in the protoplasm is calculated to be about 0.7. This is quite similar to the coefficient suggested by Robinson and Stokes (1970). The concentration of Cl^- in cytoplasm of *Chara australis* is about 20 mM (Tazawa et al., 1974). The passive channel conductance g_d is approximately the sum of the Cl^- channel conductance g_{Cl} and the K^+ channel conductance g_K (Eq. 6) and the emf is the weighted average of two emf's, i.e., K^+ channel E_K, and Cl^- channel E_{Cl} (Eq. 7).

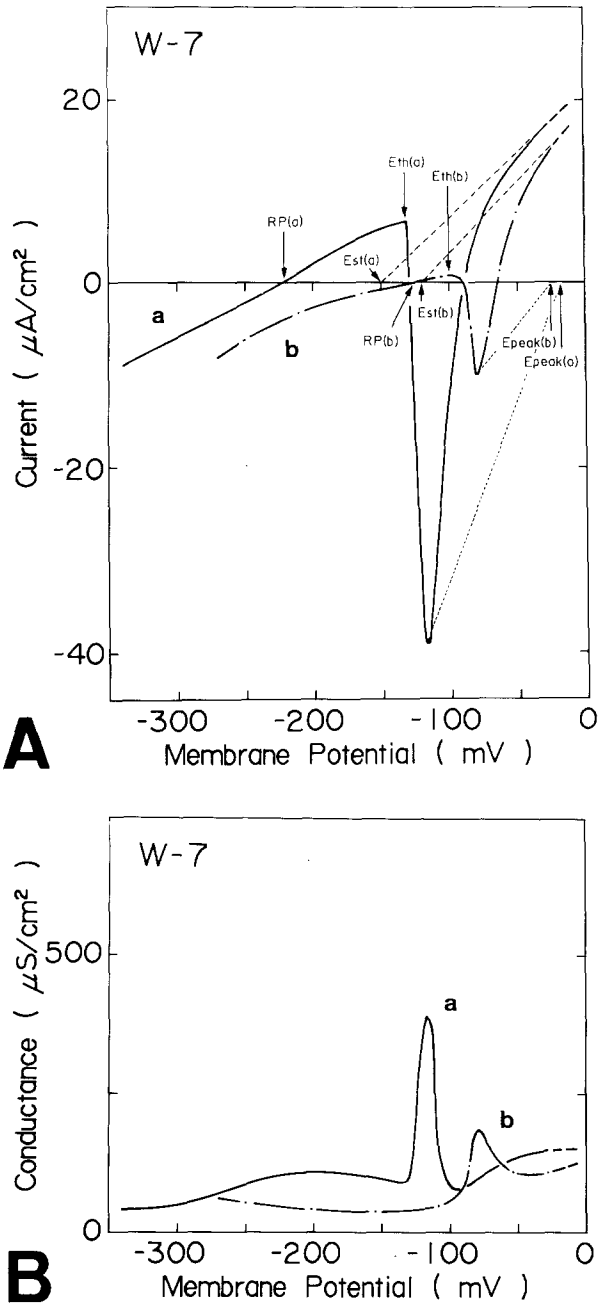

Fig. 7. (*A*) Changes of *I/V* curve with 20 μM W-7. The I/V curves obtained before (*a*) and 50 min after (*b*) the application of W-7. The resting potential depolarized markedly (RP(b)) in *b*. The transient inward current decreased markedly and the threshold level (Eth(b)) shifted to a less negative level in *b*. The emf of region III(Est) is about −140 mV in *a* and −120 mV in *b*. (*B*) The *G/V* curves obtained before (*a*) and 50 min after (*b*) application of W-7 (20 μM). The smaller conductance peak at around −200 mV corresponds to the peak conductance of H^+ pump, while the larger one at around −100 mV to that of the passive excitatory channel. Both conductance peaks reduced markedly in *b*. The conductance of the late steady high conductance region, where the voltage is less negative than −50 mV was not much affected by EGTA in *b*.

$$g_d = g_{Cl} + g_K \quad (6)$$

$$E = (g_{Cl}E_{Cl} + g_K E_K)/g_d. \quad (7)$$

Then, Nernst potentials E_K and E_{Cl} are calculated to be about −120 and 84 mV, respectively. Thus, the emf (E_{peak}) at the peak of the transient inward current or at the peak of action potential should be somewhere between E_{Cl} and E_K. Then, if the Cl^- channel alone is partially inhibited, the shift of emf peak (E_{peak}) to a more negative level is expected (Eq. 7). On the other hand, if K^+ channel alone is partially inhibited, shift of E_{peak} to a less negative level is expected (Eq. 7). Actually a marked decrease of the transient inward current and a slight shift of E_{peak} to a more negative level were observed at the early stage of La^{3+} treatment (Fig. 5*A*). External application of EGTA had almost the same effect (Fig. 6*A*). Since, external application of La^{3+} or EGTA is expected to reduce the Ca^{2+} influx through the plasma membrane, the loss of the transient inward current may be triggered by the loss of Ca^{2+} influx.

In living cells internal Ca^{2+} level is supposed to be balanced between the passive influx through Ca^{2+} channel and some active extruding pumping systems (*see* review by Schatzmann, 1982). Therefore, it is quite probable that if the passive Ca^{2+} influx is inhibited by La^{3+} or by EGTA, then a decrease of internal Ca^{2+} level below 10^{-6} to 10^{-7} M is expected.

La^{3+} treatment caused EC uncoupling in *Chara* internode (Tsutsui et al., 1987). Such an EC uncoupling is also caused by the reduction of the transient increase of internal free Ca^{2+} level. The marked shift of the voltage of the peak inward current (E_{peak}) to a more negative level and deformation of action potential (Tsutsui et al., 1987) suggest that the activation of Cl^- channel is not only slowed down but also markedly depressed by the decrease of Ca^{2+} influx, or by the slight decrease of internal Ca^{2+} level. Therefore, it can be concluded that the transient increase of Cl^- efflux, which is the main component of the transient inward current, is activated by the Ca^{2+} influx.

The emf in region III (Est) was primarily around −140 mV, which is about 20 mV more negative than E_K. However, the emf shifted to a less negative level (−110 to −130 mV) after the application of DCCD, La^{3+}, EGTA, TFP and W-7 (Figs. 3*A*, 4*A*, 5*A*, 6*A* and 7*A*), which is very close to the calculated E_K stated above. The pump current in the *Chara* membrane saturates at a large depolarization (Kishimoto et al., 1984). The recorded current in region III under the ramp voltage clamp is the sum of the saturated outward pump current and the steady outward current through the passive channel. This saturated outward H^+-pump current is expected to shift the Est toward a level more negative than E_K. The extent of this shift can be calculated with Eq. (5). The pump conductance (g_p) at largely depolarized state is about 30 to 40 $\mu S/cm^2$ and pump emf (E_p) is about −230 mV (Kishimoto et al., 1984). The passive channel at such a depolarized voltage consists mainly of opened K^+ channel as described above. The g_d is about 180 $\mu S/cm^2$ (Fig. 3*B*) and E_d is −120 mV (Fig. 3*A*). Then, the expected E at this voltage is around −140 mV. This is what was actually observed in the case of Est (*a*) in Figs. 3*A*, 4*A*, 5*A*, 6*A* and 7*A*. Tyerman, Findlay and Paterson (1986) studied the effect of 0.1 mM La^{3+} on *Chara inflata*. Their results showed that La^{3+} decreased the transient inward current and the late steady current in the largely depolarized region, which is very similar to our results. They suggested that La^{3+} blocked both Cl^- and K^+ channels. Since we applied only 20 μM La^{3+}, therefore we cannot exclude the possibility that more concentrated La^{3+} might attack K^+ channel as well. Takata et al. (1966) reported very similar decreases in transient inward Na^+ current and steady-state K^+ current in the lobster giant axon membrane by the external application of 11 mM La^{3+}. However, as described above, the decrease of the current in region III at the late stage of La^{3+} application is mainly caused not by the decrease of K^+ channel conductance, but by the decrease of H^+-pump conductance. These results lead to the conclusion that K^+ channel is fully opened at large depolarization even after the Ca^{2+} channel is blocked by La^{3+}. It is more likely that K^+ channel is not activated by the increase of internal Ca^{2+} level, but rather by depolarization itself.

The conductance peak around −200 mV (curve *a* in Figs. 3*B*, 4*B*, 5*B*, 6*B* and 7*B*) reflects the conductance peak of the H^+ pump (Kishimoto et al., 1984; 1985). This peak disappeared not only by DCCD (a specific inhibitor of proton-translocating ATPase), but also by La^{3+} or EGTA at the late stage of treatment. Such a reduction of Ca^{2+} level seems to closely correlate with the EC uncoupling (Tsutsui et al., 1987) and with the suppression of the H^+-pump activity. Indeed, the H^+-pump activity and excitability of the *Chara* plasmalemma is suppressed considerably by the internal perfusion with 5 mM EGTA (*unpublished*). On the other hand, internal perfusion with more concentrated Ca^{2+} (> 10^{-4} M) deteriorates the H^+ extrusion mechanism (Lühring & Tazawa, 1985) and also causes some qualitative changes in the passive channels. These results suggest that the normal H^+-pump activity is

regulated within a comparatively narrow range of internal Ca^{2+} level.

Calmodulin is one of the intracellular Ca^{2+} receptors which plays a pivotal role in many physiological regulations (Cheung, 1980). Two different types of calmodulin antagonists (W-7 and TFP) caused a marked depression of transient inward current (Figs. 6*A* and 7*A*) and also inhibition of H^+-pump activity (Figs. 6*B* and 7*B*). Marked decrease of the size of action potential reported by Beilby and MacRobbie (1984) and Tsutsui et al. (1987) in *Chara* internodes was closely related to this depression. These results are very similar to those of the effect of La^{3+} or EGTA. Thus, these suggest the considerable suppression of the activation kinetics of the Cl^- channel. The activation of the Cl^- channel may be primarily triggered by the slight increase of internal Ca^{2+} level, which is caused by the influx of Ca^{2+} through the Ca^{2+} channel. Therefore, a Ca^{2+}-calmodulin system is likely involved somewhere between Ca^{2+} channel and Cl^- channel. The inhibitory effect of TFP on the pump activity is also suggested by Beilby and MacRobbie (1984). At present we have no detailed information on the possibility of H^+-pump regulation by a Ca^{2+} calmodulin system. However, it is quite probable that such a system is also regulated with a comparatively narrow range of internal Ca^{2+} level.

References

Beilby, M.J., Coster, H.G.L. 1979. The action potential in *Chara corallina*. II. Two activation-inactivation transients in voltage clamps of the plasmalemma. *Aust. J. Plant Physiol.* **6**:323–335

Beilby, M.J., MacRobbie, A.C. 1984. Is calmodulin involved in electrophysiology of *Chara corallina? J. Exp. Bot.* **153**:568–580

Boron, W.F., Russell, J.M., Brodwick, M.S., Keifer, D.W., Roos, A. 1978. Influence of cyclic AMP on intracellular pH regulation and chloride fluxes in barnacle muscle fibers. *Nature (London)* **276**:511–513

Cheung, W.Y. 1980. Calmodulin plays a pivotal role in cellular regulation. *Science* **207**:19–27

Findlay, G.P., Hope, A.B. 1964. Ionic relations of cells of *Chara australis*. IX. Analysis of transport membrane currents. *Aust. J. Biol. Sci.* **17**:400–411

Gaffey, C.T., Mullins, L.J. 1958. Ion fluxes during the action potential in *Chara*. *J. Physiol. (London)* **144**:505–524

Hager, A., Menzel, H., Krauss, A. 1971. Versuche und hypothese zur primärwirkung des auxins beim streckungswachstum. *Planta* **100**:47–75

Hayama, T., Shimmen, T., Tazawa, M. 1979. Participation of Ca^{2+} in cessation of cytoplasmic streaming induced by membrane excitation in *Characeae* internodal cells. *Protoplasma* **99**:305–321

Hidaka, H., Tanaka, T. 1983. Naphthalenesulfonamides as calmodulin antagonists. *Methods Enzymol.* **102**:185–194

Kikuyama, M., Tazawa, M. 1983. Transient increase of intracellular Ca^{2+} during excitation of tonoplast free *Chara* cells. *Protoplasma* **117**:62–67

Kishimoto, U. 1961. Current voltage relations in *Nitella*. *Biol. Bull. (Woods Hole)* **121**:370

Kishimoto, U. 1964. Current voltage relations in *Nitella*. *Jpn. J. Physiol.* **14**:515–527

Kishimoto, U. 1965. Voltage clamped internal perfusion studies on *Nitella* internodes. *J. Cell Comp. Physiol.*, Suppl. 2 **66**:43–54

Kishimoto, U. 1968. Electromotive force of *Nitella* membrane during excitation. *Jpn. J. Physiol.* **9**:539–551

Kishimoto, U., Kami-ike, N., Takeuchi, Y. 1981. A quantitative expression of the electrogenic pump and its possible role in the excitation of *Chara* internodes. *In:* The Biophysical Approach to Excitable Systems. W.J. Adelman, Jr., and D.E. Goldman, editors. pp. 165–181. Plenum, New York, London

Kishimoto, U., Kami-ike, N., Takeuchi, Y., Ohkawa, T. 1984. A kinetic analysis of the electrogenic pump of *Chara corallina*. I. Inhibition of the pump by DCCD. *J. Membrane Biol.* **80**:175–183

Kishimoto, U., Takeuchi, Y., Ohkawa, T., Kami-ike, N. 1985. A kinetic analysis of the electrogenic pump of *Chara corallina*. III. Pump activity during action potential. *J. Membrane Biol.* **86**:27–36

Kitasato, H. 1973. K permeability of *Nitella clavata* in the depolarized state. *J. Gen. Physiol.* **62**:535–549

Lettvin, J.Y., Pickard, W.F., McCulloth, W.S., Pitts, W. 1964. A theory of passive flux through axon membrane. *Nature (London)* **202**:1338–1339

Levin, R.M., Weiss, B. 1976. Mechanism by which phychotropic drugs inhibit adenosine cyclic 3′,5′-monophosphate phosphodiesterase of brain. *Mol. Pharmacol.* **12**:581–589

Lühring, H., Tazawa, M. 1985. Effects of cytoplasmic Ca^{2+} on the membrane potential and membrane resistance of *Chara* plasmalemma. *Plant Cell Physiol.* **26**:635–646

Lunevsky, V.Z., Zherelova, O.M., Vostrikov, I.Y., Berestovsky, G.N. 1983. Excitation of *Characeae* cell membranes as a result of activation of calcium and chloride channels. *J. Membrane Biol.* **72**:43–58

Mailman, D.S, Mullins, L.J. 1965. The electrical measurement of chloride fluxes in *Nitella*. *Aust. J. Biol. Sci.* **19**:385–398

Mullins, L.J. 1962. Efflux of chloride ions during action potential of *Nitella*. *Nature (London)* **196**:986–987

Oda, K. 1976. Simultaneous recording of potassium and chloride effluxes during an action potential in *Chara corallina*. *Plant Cell Physiol.* **17**:1085–1088

Ohkawa, T., Kishimoto, U. 1974. The electromotive force of the *Chara* membrane during the hyperpolarizing response. *Plant Cell Physiol.* **15**:1039–1054

Ohkawa, T., Kishimoto, U. 1977. Breakdown phenomena in the *Chara* membrane. *Plant Cell Physiol.* **18**:67–80

Reeves, M., Shimmen, T., Tazawa, M. 1985. Ionic activity gradients across the surface membrane of cytoplasmic droplets prepared from *Chara australis*. *Plant Cell Physiol.* **26**:1185–1193

Robinson, R.A., Stokes, R.H. 1970. Electrolyte Solutions. 2nd Ed. Butterworth, London

Sanders, D. 1980. The mechanism of Cl^- transport at the plasma membrane of *Chara corallina*. I: Cotransport with H^+. *J. Membrane Biol.* **53**:129–141

Schatzmann, H.J. 1982. Penetration of calcium through the membrane of excitable cells. *In:* Membrane Transport of Calcium. E. Carafoli, editor. pp. 41–108. Academic, London

Sze, H. 1985. H^+-translocating ATPases: Advances using membrane vesicles. *Annu. Rev. Plant Physiol.* **36:**175–208

Takata, M., Pickard, W.F., Lettvin, J.Y., Moore, J.W. 1966. Ionic conductance changes in lobster axon membrane when lanthanum is substituted for calcium. *J. Gen. Physiol.* **50:**461–471

Takeuchi, Y., Kishimoto, U., Ohkawa, T., Kami-ike, N. 1985. A kinetic analysis of the electrogenic pump of *Chara corallina*. II. Dependence of the pump activity on external pH. *J. Membrane Biol.* **86:**17–26

Tazawa, M., Kishimoto, U., Kikuyama, M. 1974. Potassium, sodium and chloride in the protoplasm of characeae. *Plant Cell Physiol.* **15:**103–110

Tsutsui, I., Ohkawa, T., Nagai, R., Kishimoto, U. 1987. Role of calcium ion in the excitability and electrogenic pump activity of the *Chara corallina* membrane: I. Effects of La^{3+}, verapamil, EGTA, W-7, and TFP on the action potential. *J. Membrane Biol.* **96:**65–73

Tyerman, S.D., Findlay, G.P., Paterson, G.J. 1986. Inward membrane current in *Chara inflata:* II. Effects of pH, Cl^--channel-blockers and NH_4^+, and significance for the hyperpolarized state. *J. Membrane Biol.* **89:**153–162

Williamson, R.E., Ashley, C.C. 1982. Free Ca^{2+} and cytoplasmic streaming in the alga *Chara*. *Nature (London)* **296:**647–651

Received 17 September 1986; revised 9 December 1986